

# Preparation and performance of an advanced multiphase composite ceramic material

Chonghai Xu\*

*Department of Mechanical and Electronic Engineering, Shandong Institute of Light Industry, Jinan, 250100, PR China*

Received 9 October 2003; received in revised form 30 March 2004; accepted 10 April 2004

Available online 15 June 2004

## Abstract

According to the optimum composition achieved from the material design, an advanced 15 vol.% SiC and 15 vol.% Ti(C,N) containing alumina-based multiphase ceramic material with good comprehensive mechanical properties has been fabricated with hot pressing technique. Only under suitable hot pressing conditions and material compositions can better microstructures and mechanical properties be achieved. The optimum hot pressing parameters for the SiC/Ti(C,N)/Al<sub>2</sub>O<sub>3</sub> material are as follows: the hot pressing temperature is 1780 °C, the time duration equals to 60 min and the pressure remains 35 MPa. The content of each dispersed SiC and Ti(C,N) phase has significant effects not only on the mechanical properties but on the engineering performances of the ceramic materials. Good wear resistance is found for the kind of ceramic material when used as cutting tools in the machining of the hardened carbon steel. Failure mechanisms are mainly the abrasive wear and the adhesive wear. The developed SiC/Ti(C,N)/Al<sub>2</sub>O<sub>3</sub> multiphase ceramic material will be well used as the structural parts with the requirement of high wear resistance such as cutting tools.

© 2004 Elsevier Ltd. All rights reserved.

**Keywords:** Microstructure; Mechanical properties; Cutting tools; Wear resistance; SiC/Ti(C,N)/Al<sub>2</sub>O<sub>3</sub>

## 1. Introduction

Multiphase composite is one of the important developing trends of the advanced structural ceramic materials in the 21st century.<sup>1,2</sup> The trend of ceramic material researches from monolithic phase to multiphase will provide wider space for the consideration of the ceramic material design. Considerable improvement in mechanical properties of the single phase ceramic materials has been achieved by incorporating one or more other components into the base material to form ceramic matrix composites (CMCs). The reinforcing component is often in the form of particles or whiskers, such as TiC, TiN, TiB<sub>2</sub>, SiC particulate, SiC whisker, B<sub>4</sub>C, ZrO<sub>2</sub>, WC, (W,Ti)C, Ti(C,N), Cr<sub>3</sub>C<sub>2</sub>, NbC, etc.<sup>3–7</sup> Ceramic composites are of increasing interest with oxide matrices, particularly alumina being dominant. However, the corresponding material compositions, the processing techniques, the reinforcing and toughening mechanisms, the properties and their application still need further study.

Till now, ceramic composites have been used widely in cutting tools, drawing or extrusion, seal rings, valve seats, bearing parts, and a variety of high temperature engine parts, etc. because of their higher wear resistance, higher thermal and chemical stability. Varieties of researches have been carried out focusing on the cutting performance, friction and wear and fracture mechanisms of ceramics when used as the tool materials in machining different work materials.<sup>8–13</sup> It is concluded that wear of ceramic tools is resulted from the combinative function of both mechanical and chemical wear. Wear mechanisms include the abrasive wear, adhesive wear, chemical wear, diffusion wear and oxidation wear, etc. Wear is not the intrinsic feature of the ceramic tool materials. It is closely related with the cutting conditions. If the tool material is different, or the cutting condition or the work material is different, the dominant wear mechanism may vary.

In the present study, according to the results of the material design in the former reports,<sup>14,15</sup> an advanced SiC and Ti(C,N) containing alumina-based multiphase ceramic material with good comprehensive mechanical properties has been manufactured using the hot pressing technique. The microstructure and the engineering performance of the material are also studied in detail.

\* Tel: +86 531 8619858/8556865; fax: +86 531 8968495.

E-mail address: [xch@sdili.edu.cn](mailto:xch@sdili.edu.cn) (C. Xu).

## 2. Experimental procedures

High purity  $\text{Al}_2\text{O}_3$ ,  $\beta\text{-SiC}$  and  $\text{Ti}(\text{C},\text{N})$  powders were used as the starting materials with sizes of 0.8, 1.0 and  $1.0\ \mu\text{m}$ , respectively. Before mixing, all the powders had to be cleaned with the hot diluted  $\text{HNO}_3$  and  $\text{NaOH}$  solution in order to reduce the effect of the impurities. Then,  $\text{Al}_2\text{O}_3$  was blended with  $\text{SiC}$  and  $\text{Ti}(\text{C},\text{N})$  and doped with different amounts of sintering additives. The mixtures were subsequently homogenized with absolute alcohol media in a ball mill for 80 h. After milling, the slurry was screened in nitrogen and dried in vacuum. Samples were then formed by hot pressing (HP) technique in  $\text{N}_2$  atmosphere in a graphite mould. Sintered bodies were then cut with a diamond wheel into specimens and inserts.

Relative density of the sample was measured by Archimedes' technique. The three point bending method was used to measure the flexural strength with a span of 20 mm and a cross head speed of 0.5 mm/min. The test bars were carefully ground and polished into the size of 3 mm thick, 4 mm wide and 30 mm long with the surface roughness less than  $0.1\ \mu\text{m}$ . The edges of the tensile surface were chamfered. The fracture toughness was determined on bars of 3 mm (thickness)  $\times$  4 mm (width)  $\times$  40 mm (length) by a four point SENB (single edge notched beam) method with a 10 mm inner span and a 20 mm outer span at a cross head speed of 0.1 mm/min. A straight notch with a ratio to thickness of about 0.5 mm was introduced at the center part of the test bar using a 0.2 mm wide diamond blade and depth of notch was about 1.5 mm. To reduce the effect of a finite notch tip radius on the initial crack propagation, the bottom portion of the saw notch was sharpened by using a sharp razor blade that had been sprinkled with  $1\ \mu\text{m}$  diamond paste. This double notch procedure allowed the notch radius to be reduced up to  $<10\ \mu\text{m}$ . Hardness was measured with a Vickers hardness tester (model HV-120) with a static load of 196 N and a holding time of 15 s. Data for density, flexural strength, fracture toughness and hardness were gathered on five specimens.

Microstructures of the material were observed with scanning electronic microscope (SEM, model HITACHI S-570). Samples used for the analyses with transmission electron microscope (TEM) were first ground and polished mechanically to be less than  $50\ \mu\text{m}$ , and then ion thinned to perforation. Microstructural characterizations of the material were performed with TEM (model HITACHI H-800) equipped with the energy spectrum and operated at 175 kV. X-ray diffraction (XRD, model D/max-2400) was used for the phase

Table 1

Machining parameters used in the cutting tests

Group number	Cutting speed, $v$ (m/min)	Feed rate, $f$ (mm/rev)	Depth of cut, $a_p$ (mm)
1	90	0.2	1.0
2	150	0.2	1.0
3	220	0.15	0.6

analysis of the sintered samples with the scanning speed of  $4^\circ/\text{min}$ , the working voltage of 44 kV and the electric current of 150 mA.

The developed ceramic material was then utilized as a tool material, and cutting tests were done according to the following cutting conditions. Continuous turning experiments were carried out on a lathe (model CA6140) equipped with a  $45^\circ$  lead angle,  $5^\circ$  negative inclination,  $5^\circ$  negative rake tool holder,  $5^\circ$  clearance and dry cut. The geometry of the tool inserts is SNGN160603 with an edge chamfer of 0.2 mm at  $20^\circ$ . The work material is a 0.45% C mild carbon steel (#45 steel) with a hardness of 40–42 HRC in the form of round bars. Machining parameters are given in Table 1. Here AST is used to indicate the  $\text{SiC}/\text{Ti}(\text{C},\text{N})/\text{Al}_2\text{O}_3$  series ceramic materials. AS15T15, AS10T10 and AS10T30 indicates the  $\text{SiC}/\text{Ti}(\text{C},\text{N})/\text{Al}_2\text{O}_3$  ceramic material with 15 vol.%  $\text{SiC}$  and 15 vol.%  $\text{Ti}(\text{C},\text{N})$ , 10 vol.%  $\text{SiC}$  and 10 vol.%  $\text{Ti}(\text{C},\text{N})$ , 10 vol.%  $\text{SiC}$  and 30 vol.%  $\text{Ti}(\text{C},\text{N})$ , respectively. A0 indicates the pure alumina ceramic. In order for the comparison,  $\text{Al}_2\text{O}_3/30\ \text{vol.}\% (\text{W},\text{Ti})\text{C}$  ceramic composite was also fabricated with the same technique, which is marked as AW30.

## 3. Results and analyses

### 3.1. Processing technology

The results of the chemical analysis of the used powders are shown in Table 2. Since small quantities of impurities like Fe,  $\text{Fe}_2\text{O}_3$ , etc. resulted from the incomplete chemical reaction and other production stages of the raw materials, have been mixed into these ceramic powders, all the powders have to be washed before use with the hot diluted  $\text{HNO}_3$  and  $\text{NaOH}$  solution in order to reduce the impurities.

Although results of the technological design of the ceramic material suggest that the pressure should be the higher the better,<sup>15</sup> the pressure used in the present study is 35 MPa limited by the strength of the graphite mould at elevated

Table 2

Results of the chemical analyses of the ceramic powders (%)

Material	N	C	$\text{Fe}_2\text{O}_3$	$\text{TiO}_2$	CaO	$\text{C}_f$	Fe	$\text{K}_2\text{O}$	$\text{Na}_2\text{O}$	O
$\text{Al}_2\text{O}_3$	–	–	0.020	0.038	0.163	–	–	0.005	0.039	–
$\text{SiC}$	–	–	–	–	–	$<0.3$	$<0.2$	–	–	$<0.8$
$\text{Ti}(\text{C},\text{N})$	$>10.8$	9.2–10.1	–	–	–	$<0.3$	$<0.2$	–	–	$<0.7$

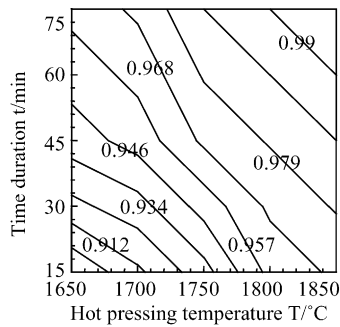


Fig. 1. Variation of the relative density of AS15T15 ceramic material with the hot pressing parameters.

temperature. Figs. 1 and 2 indicates the effect of hot pressing temperature and time duration on the relative density and the fracture toughness of AS15T15 ceramic material, respectively. It seems that when the hot pressing temperature is 1780 °C and the time duration equals to 60 min, the relative density of the material can reach about 98% and the fracture toughness is higher than 5.2 MPa m<sup>1/2</sup>. With these processing parameters, the other mechanical properties such as the flexural strength and the hardness are all relatively high. The experimental results coincide well with that of the technological design.<sup>15</sup> However, both the hot pressing temperature and the time duration that are needed to reach the same density of the SiC containing Alumina ceramic is higher and longer than that of the corresponding ceramic material without SiC addition. The main reason consists in that the covalent bond compound SiC is more difficult to be sintered than other ionic and metallic bond compounds such as TiC and ZrO<sub>2</sub>, etc. Analysis with XRD denotes that the material after sintering keeps the same composition with that before sintering and no new phases are found to exist inside the AS15T15 material (Fig. 3).

### 3.2. Microstructure and mechanical property

According to the former study,<sup>14</sup> comprehensive mechanical properties will be achieved for the SiC/Ti(C,N)/Al<sub>2</sub>O<sub>3</sub> ceramic material when the volume fraction of both SiC and Ti(C,N) is nearly 15% and when the hot pressing tempera-

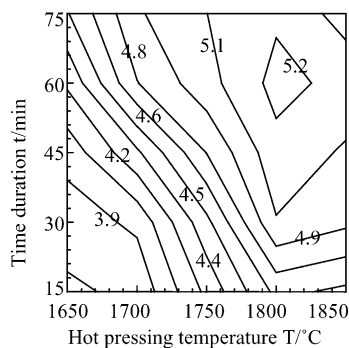


Fig. 2. Variation of the fracture toughness of AS15T15 ceramic material with the hot pressing parameters (unit of fracture toughness is MPa m<sup>1/2</sup>).

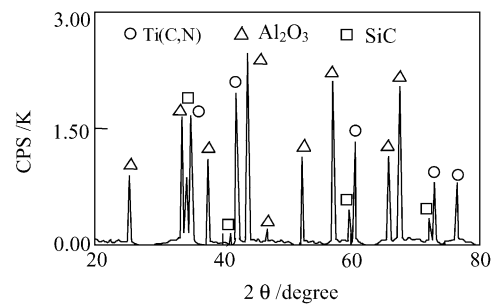


Fig. 3. XRD analysis of the sintered AS15T15 ceramic material.

ture, the time duration and the pressure is 1780 °C, 60 min and 35 MPa, respectively. The flexural strength, the fracture toughness and the hardness of AS15T15 ceramic material is measured to be 721 MPa, 5.4 MPa m<sup>1/2</sup> and 18.97 GPa, respectively, which is 43.9, 42.1 and 4.6%, respectively, higher than that of the pure alumina ceramic. Mechanical properties of all the selected ceramic materials are listed in Table 3.

The hot pressing parameters have significant effect on the microstructure and the mechanical property of the ceramic materials. Under the condition of 1700 °C × 30 min, the fracture surface of the sample is relatively smooth which corresponds to the flexural strength of 561 MPa and the fracture toughness of 3.9 MPa m<sup>1/2</sup>. But when the hot pressing temperature is 1780 °C and the time duration is 60 min, the fracture surface of the sample is noticeably accented (Fig. 4a). The flexural strength has correspondingly reached 721 MPa and the fracture toughness 5.4 MPa m<sup>1/2</sup>. The first reason is the increase of the relative density which is increased from approximately 93% at conditions of 1700 °C × 30 min to 98% at 1780 °C × 60 min. The second reason is that affected by the internal residual thermal stress field, the dispersed SiC and Ti(C,N) grains interact with the propagating cracks which results in the crack deflection, crack bridging or grain pulling-out (Fig. 4b and c). Thus, the crack path is extended and the flexural strength and the fracture toughness are then increased. Furthermore, different extent of brittle cleavage may happen in the fracture process in some alumina grains resulted from the complex residual thermal stresses around the grains. The complex cleavage surface is then formed with obvious features of the pulling-out effect of grains (Fig. 4d). As a result, the energy of fracture is increased and both fracture toughness and flexural strength are subsequently enhanced.

Table 3  
Mechanical properties of the selected ceramic materials at hot pressing conditions of 1780 °C × 60 min × 35 MPa

Material	Flexural strength, $\sigma_f$ (MPa)	Fracture toughness, $K_{IC}$ (MPa m <sup>1/2</sup> )	Vickers hardness, $H_V$ (GPa)
AS15T15	721	5.4	18.97
AS10T10	697	5.2	18.79
AS10T30	660	5.0	18.82
A0	501	3.8	18.1
AW30	765	5.1	18.92

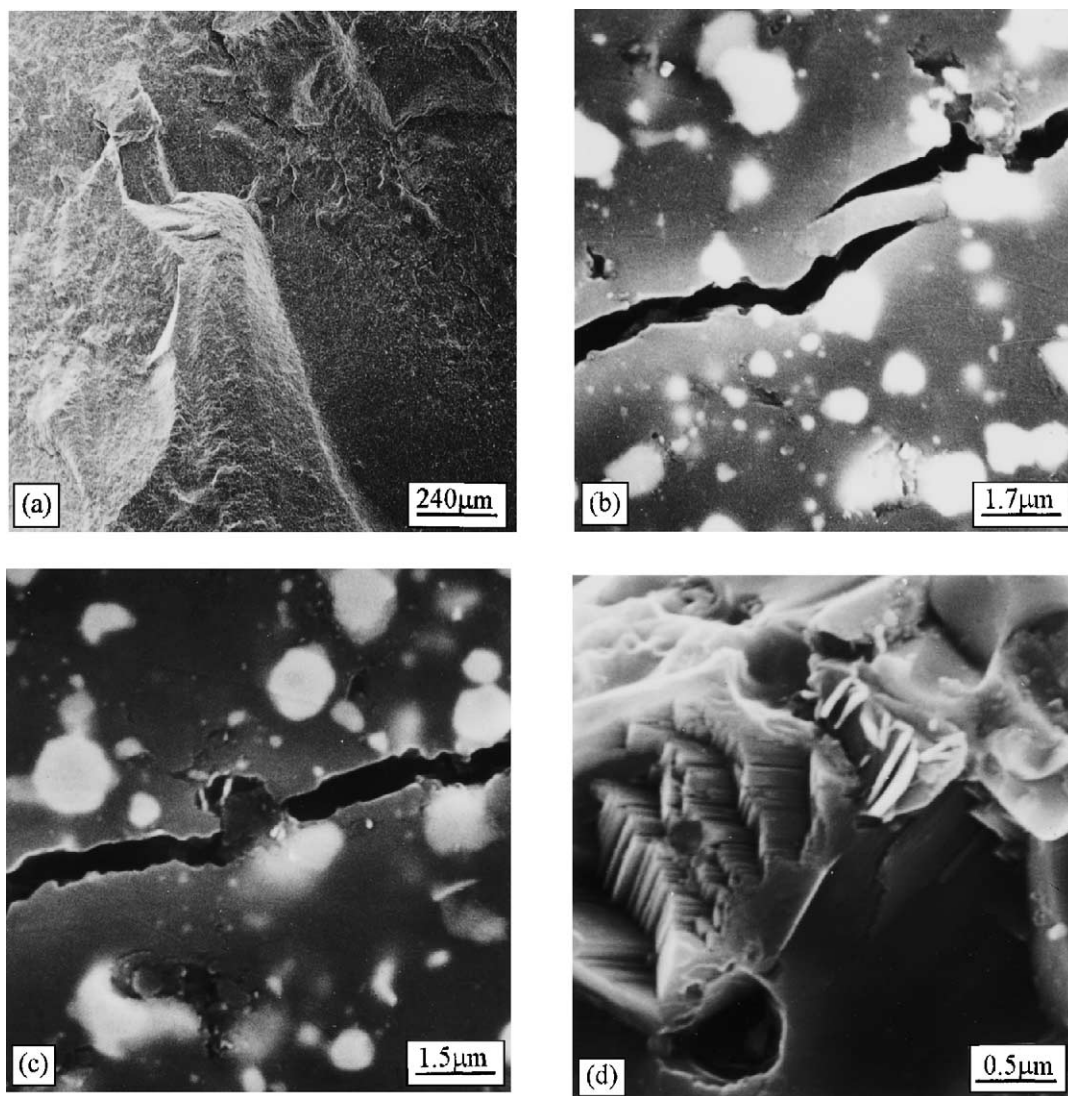


Fig. 4. Fracture morphology of AS15T15 ceramic material at 1780 °C × 60 min (a) accidented fracture surface; (b) crack bridging; (c) grain pulling-out; (d) brittle cleavage .

Microstructural morphology of the material under TEM is shown in Fig. 5. Both the two dispersed phases SiC and Ti(C,N), distributed uniformly in the matrix, bond well with Al<sub>2</sub>O<sub>3</sub> at the interface with fine grain size. SiC particles are usually dispersed uniformly in the matrix, but few of them with the sub-micron meter grain size, nearly less than 200 nm, can be observed to exist inside the alumina grains (Fig. 5a). These existing sub-micron meter sized SiC particles inside the alumina grains can improve the flexural strength and the fracture toughness of the material with the similar toughening mechanism of intergranular fracture happened frequently in ceramic nanocomposites.<sup>16,17</sup> On the other hand, the twin sub-structure can be observed clearly no matter inside large or small SiC grains among which the twin sub-structure with the orientation angle of 60° is discovered (Fig. 5b). The formation of twins will absorb the energy of fracture at the interface of Al<sub>2</sub>O<sub>3</sub>/SiC so that the addition of SiC can contribute not only to the reinforcement

of the material but also to the increase in the fracture toughness of the material which is similar, to a certain extent, to the toughening mechanism found in the whisker toughened ceramic material.<sup>18</sup>

Dislocations have also been observed in the SiC/Ti(C,N)/Al<sub>2</sub>O<sub>3</sub> ceramic material. Typical morphology is given in Fig. 5c. Most of the dislocations originate from the interface under the action of the residual thermal stresses and then propagate into the grains. On the one side, the elastic strain energy can be deposited in the dislocations. On the other side, when the crack reaches, the dislocations can absorb parts of the energy of fracture through their own deformation. The propagating crack will be pinned and the fracture toughness is resultedly increased. At a matter of fact, the dislocation toughening, which is similar to the microcrack toughening, can cause the regional blunting effect in the tip area of the extending crack and it will have the  $K_R$ -curve behavior.<sup>19,20</sup> The interlaced dislocation lines are seemed



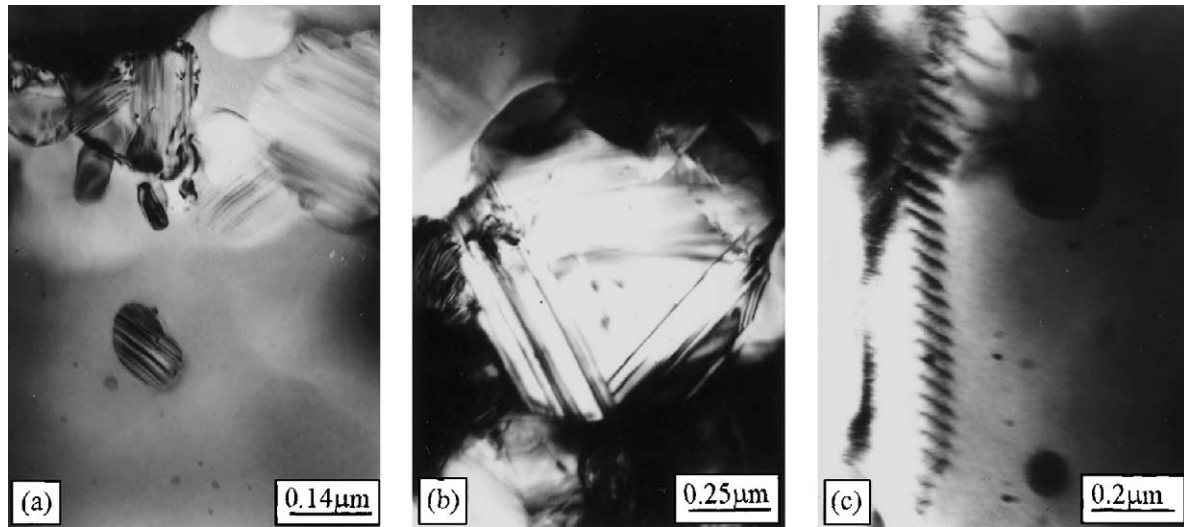


Fig. 5. TEM morphology of AS15T15 ceramic material: (a) sub-micron meter sized SiC grain; (b) twin formed in SiC grain; (c) dislocation.

to be equivalent to the second fining of the matrix grains. Since its size has reached the nano-meter degree, the effect of reinforcement on the ceramic material is self-evident.

### 3.3. Cutting performance

The flank wear curves of the selected ceramic materials when machining the hardened #45 carbon steel are given in Fig. 6 where the cutting conditions are: the cutting speed  $v = 220$  m/min, the feed rate  $f = 0.15$  mm/rev and the depth of cut  $a_p = 0.6$  mm. It seems that wear curves of all the ceramic materials obey the wear law well. But wear resistance of different ceramic materials vary with each other. Under the present experimental conditions, wear resistance of AS15T15 ceramic is higher than the other SiC/Ti(C,N)/Al<sub>2</sub>O<sub>3</sub> series ceramic materials, while is nearly the same with that of AW30 ceramic material. With the prolonging of the cutting time, the gap in the wear resistance between several ceramics is enlarged. The sequence

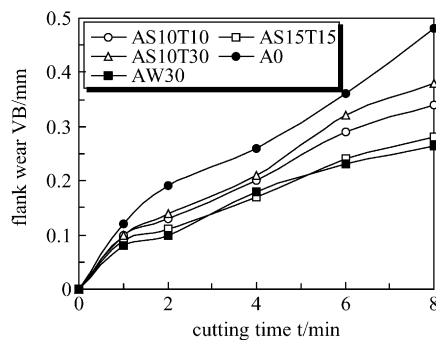
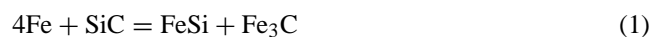


Fig. 6. Variation of the flank wear of the selected ceramic materials with the cutting time when machining the hardened #45 carbon steel with the cutting speed 220 m/min, the feed rate 0.15 mm/rev and the depth of cut 0.6 mm.

of wear resistance is  $AW30 \approx AS15T15 > AS10T10 > AS10T30 > A0$  which is nearly the same with that of the comprehensive mechanical properties (Table 3). After 8 min of machining, the flank wear resistance of AS15T15 ceramic is 21.4, 35.7 and 71.5% higher than that of AS10T10, AS10T30 and the pure Al<sub>2</sub>O<sub>3</sub> ceramic material, respectively.

Wear modes of the developed SiC/Ti(C,N)/Al<sub>2</sub>O<sub>3</sub> series ceramic materials are primarily the same, i.e., mainly the flank wear and the crater wear accompanied with slight depth of cut wear. SEM morphologies of the crater wear and the flank wear of AS15T15 ceramic material are shown as an example in Fig. 7. Under the experimental conditions, the adhesion between the tool material and the work material happens in some areas in the rake face of the tool where clumps of the adhered materials can notably be observed (Fig. 7a). The case is ceaselessly intensified with the increase in the cutting speed resulted from the high cutting temperature. In the flank wear area, main wear mode is changed from the abrasive wear at lower speed to the adhesive wear at higher speed where the plowing grooves are relatively short and shallow (Fig. 7b). Occasionally, few ceramic grains have ever been observed to break off in the flank wear area in AS10T30 ceramic material.

In fact, when machining hardened steel with SiC containing ceramic tool material, SiC will react with the iron element in the work material at high cutting temperature.<sup>10,11</sup> The following reaction is the most possible one that happens.



Thermal dynamic calculation indicates that when the cutting temperature reaches 425 K, the free energy is  $-0.112$  kJ/mol  $< 0$ , which suggests that the reaction might happen. The reaction will be intensified with the increase in the cutting temperature which is resulted from the increase in the cutting speed. The reaction will then lower the hardness

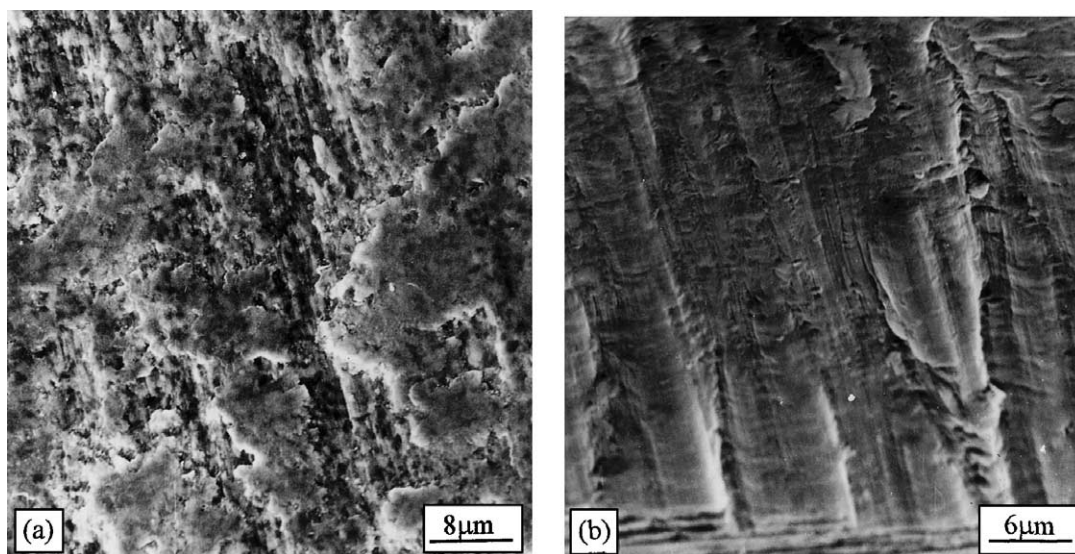


Fig. 7. Wear morphologies of AS15T15 ceramic material when machining the hardened #45 carbon steel with the cutting speed 220 m/min, the feed rate 0.15 mm/rev and the depth of cut 0.6 mm: (a) crater wear in the rake face and (b) flank wear.

and the wear resistance of SiC and weaken the bonding strength between SiC and the alumina matrix. As a result, SiC particulates will break off easily under the action of the scratching of the hard particles in the work material and the cutting performance of the ceramic tool will be lowered.

Additionally, the dissolution wear happened at elevated temperature is one of the factors that will influence the cutting performance of SiC containing ceramics. Brandt<sup>21</sup> pointed out that the solubility of iron in SiC at elevated temperature is two orders of magnitude higher than that in TiC. The increase of the content of iron element in the ceramic tool material will intensify the adhesion between the tool and the work material, which will lead to the lower cutting performance.

But on the other hand, since the free energy of formation of Ti(C,N) is lower than other hard carbides such as TiC and WC, it has higher chemical stability and is difficult to react with the work material. Ti(C,N) is known as possessing higher crater wear resistance and higher adhesion wear resistance through the effective prevention of the diffusion between the tool and work material.<sup>22,23</sup> As an integrated result, SiC/Ti(C,N)/Al<sub>2</sub>O<sub>3</sub> ceramic material still reveals good cutting performance.

#### 4. Conclusions

An advanced SiC/Ti(C,N)/Al<sub>2</sub>O<sub>3</sub> multiphase ceramic material has been developed by means of the hot pressing technique with the flexural strength, the fracture toughness and the hardness of 721 MPa, 5.4 MPa m<sup>1/2</sup> and 18.97 GPa, respectively. The optimum processing parameters for the material are that the hot pressing temperature is 1780 °C, the time duration is 60 min and the pressure is 35 MPa. Quantities of twins and dislocations are observed to exist in

the material, which can undoubtedly contribute to the toughening and strengthening of the ceramic material. When the developed material is used as a tool material in the machining of the hardened #45 carbon steel, its wear resistance is 71.5% higher than that of the pure alumina ceramics.

#### Acknowledgements

The Foundation for University Key Teacher by the Ministry of Education, China, the Research Fund for the Excellent Young & Middle-aged Scientists, Shandong Province, the Natural Science Fund, Shandong Province, are all greatly appreciated for supporting this project.

#### References

- Guo, J. K., The frontiers of research on ceramic science. *J. Solid State Chem.* 1992, **69**, 108–112.
- Evans, A. G., Perspective on the development of high toughness ceramics. *J. Am. Ceram. Soc.* 1990, **73**, 187–195.
- Fu, Y., Gu, Y. W. and Du, H., SiC whisker toughened Al<sub>2</sub>O<sub>3</sub>–(Ti,W)C ceramic matrix composites. *Scripta Materialia* 2001, **44**, 111–116.
- Gong, J., Miao, H. and Zhao, Z., The influence of TiC-particle-size on the fracture toughness of Al<sub>2</sub>O<sub>3</sub>–30 wt. TiC composites. *J. Eur. Ceram. Soc.* 2001, **21**, 2377–2381.
- Peillon, F. C. and Thevenot, F., Microstructural designing of silicon nitride related to toughness. *J. Eur. Ceram. Soc.* 2002, **22**, 271–278.
- Acchar, W., Greil, P., Martinelli, A. E. *et al.*, Effect of Y<sub>2</sub>O<sub>3</sub> addition on the densification and mechanical properties of alumina-niobium carbide composites. *Ceram. Int.* 2001, **27**, 225–230.
- Rak, Z. S. and Czechowski, J., Manufacture and properties of Al<sub>2</sub>O<sub>3</sub>–TiN particulate composites. *J. Eur. Ceram. Soc.* 1998, **18**, 373–380.
- Xu, C., Ai, X. and Huang, C., Fabrication and performance of an advanced ceramic tool material. *Wear* 2001, **249**, 503–508.

9. Barry, J. and Byrne, G., Cutting tool wear in the machining of hardened steels—Part I: alumina/TiC cutting tool wear. *Wear* 2001, **247**, 139–151.
10. Novak, S., Kalin, M. and Kosmac, T., Chemical aspects of wear of alumina ceramics. *Wear* 2001, **250**, 318–321.
11. Lo Casto, S., Lo Valvo, E., Lucchini, E. *et al.*, Ceramic materials wear mechanisms when cutting nickel-based alloys. *Wear* 1999, **225–229**, 227–233.
12. Lo Casto, S., Lo Valvo, E., Lucchini, E. *et al.*, Wear rates and wear mechanisms of alumina-based tools cutting steel at a low cutting speed. *Wear* 1997, **208**, 67–72.
13. Zhao, X., Liu, J., Zhu, B. *et al.*, Wear behavior of  $\text{Si}_3\text{N}_4$  ceramic cutting tool material against stainless steel in dry and water-lubricated conditions. *Ceram. Int.* 1999, **25**, 309–315.
14. Xu, C. and Ai, X., Multiphase tailoring and design of an advanced ceramic material. *Key Eng. Mater.* 2004, **259–260**, 112–116.
15. Xu, C. and Ai, X., Computer simulation of the densification kinetics in the fabrication of ceramic composites with hot pressing technique. *Model. Meas. Control A* 2001, **74**, 45–54.
16. Oh, Y.-S., Kim, C.-S., Lim, D.-S. *et al.*, Fracture strengths and microstructures of  $\text{Si}_3\text{N}_4/\text{SiC}$  nanocomposites fabricated by in-situ process. *Scripta Materialia* 2001, **44**, 2079–2081.
17. Tan, H. L. and Yang, W., Toughening mechanisms of nano-composite ceramics. *Mech. Mater.* 1998, **30**, 111–123.
18. Rachman, C., Mechanical properties and microstructure of whisker reinforced  $\text{Al}_2\text{O}_3$  matrix composite. *J. Am. Ceram. Soc.* 1989, **72**, 1636–1640.
19. Evans, A. G. and Faber, K. T., Crack growth resistance of microcracking brittle materials. *J. Am. Ceram. Soc.* 1984, **67**, 255–258.
20. Sigl, L. S. and Kleebe, H. J., Microcracking in  $\text{B}_4\text{C}-\text{TiB}_2$  composites. *J. Am. Ceram. Soc.* 1995, **78**, 2374–2380.
21. Brandt, G., Flank and crater wear mechanisms of  $\text{Al}_2\text{O}_3$  based cutting tools when machining steel. *Wear* 1989, **112**, 39–43.
22. Ettmayer, P., Kolaska, H., Lengauer, W. *et al.*, Ti(C,N) cermets: metallurgy and properties. *Int. J. Refract. Metals Hard Mater.* 1995, **13**, 343–351.
23. Porat, R., New cutting materials based on titanium carbonitride. *Mod. Dev. Powder Metallurg.* 1988, **19**, 345–365.